

# Computer Simulation of the Stability of Water Clusters Containing Nitrogen Oxide Molecules

A. E. Galashev and V. N. Chukanov

*Institute of Industrial Ecology, Ural Division, Russian Academy of Sciences,  
ul. Sof'i Kovalevskoi 20a, Yekaterinburg, 620219 Russia*

Received February 27, 2004

**Abstract**—The stability of water clusters containing nitrogen oxide molecules is studied by the molecular dynamics method. The composition and size of thermodynamically stable heteroclusters are determined. The inclusion of two molecules of nitrogen oxide into aggregates containing seven or more water molecule increases the cluster stability. The correlation between the stability of heteroclusters and the ratio of self-diffusion coefficients of molecules of different kinds is observed. The real part of the cluster permittivity is maximal in the vicinity of the frequency of  $200\text{ cm}^{-1}$ . The inclusion of nitrogen oxide molecules into water clusters increases the characteristic frequency of dielectric relaxation. In general, heteroclusters are more stable with respect to perturbations caused by an external electric field than *pure* clusters with the same number of water molecules. The clusterization of water vapors accompanied by absorption of polar molecules of impurity favors a decrease in the greenhouse effect.

## INTRODUCTION

Nitrogen oxide  $\text{N}_2\text{O}$  is the greenhouse gas. The proportion of  $\text{N}_2\text{O}$  in the emission of greenhouse gases is only second for  $\text{CO}_2$  and  $\text{CH}_4$ . Cleaning of the Earth's atmosphere occurs due to the circulation of water. During the atmospheric residence, finely dispersed aqueous medium absorbs some portion of tropospheric gases that return to the Earth as atmospheric precipitation. The amount of various chemical elements in precipitation depends on the degree of their entrapment by water clusters and on the stability of heteroclusters formed on this basis. The ability of clusters to further growth is determined by their stability. When falling into zones of decreased temperature, stable water clusters entrapping impurity grow into droplets, snowflakes, and hailstones and precipitate on the Earth's surface. The state of clusters in the atmosphere depends not only on temperature and pressure, but also on the effect of electromagnetic fields.

The aim of this work is to study the possibility of the absorption of  $\text{N}_2\text{O}$  molecules by small water clusters, to investigate the thermodynamic and dielectric stability of clusters that captured molecules, and to determine the minimal size of a stable heterocluster and the reasons responsible for the stability of small heteromolecular aggregates.

## CRITERIA OF CLUSTER STABILITY

Maximum entropy or minimum of one of thermodynamic potentials correspond to the thermodynamic stability. The most important isodynamic stability coeffi-

cients are the following combinations [1]:  $\frac{T}{c_p}$ ,  $-\left(\frac{\partial P}{\partial V}\right)_T$ ,

$\frac{1}{\chi_{P,T}}$ , and  $\frac{1}{\epsilon_{P,T}}$ , where  $T$  is the temperature,  $P$  is the pressure,  $V$  is the volume of a system,  $c_p$  is its heat capacity at constant pressure, and  $\chi$  and  $\epsilon$  are the magnetic and dielectric permittivities, respectively. Subscripts  $P$  and  $T$  at  $\chi$  and  $\epsilon$  values indicate that the double differentiation of internal energy  $U$  with respect to magnetic  $\mathbf{B}$  and electrostatic  $\mathbf{I}$  inductions is performed

at constant pressure and temperature:  $\left(\frac{\partial^2 U}{\partial \mathbf{B}^2}\right)_{P,T} = \frac{1}{\chi_{P,T}}$

and  $\left(\frac{\partial^2 U}{\partial \mathbf{I}^2}\right)_{P,T} = \frac{1}{\epsilon_{P,T}}$ . Thermal and mechanical criteria of stability are written in the form of the following inequalities:

$$\frac{T}{c_p} > 0, \quad (1)$$

$$-\left(\frac{\partial P}{\partial V}\right)_T = \frac{1}{\beta_T V} > 0. \quad (2)$$

Criteria (1) and (2) can be used for the analysis of the stability of extended system and the system with the limited degrees of freedom. However, in the case of very small systems such as clusters, the main criterion is the inequality [2]

$$\left(\frac{\partial^2 G}{\partial n^2}\right)_{P,T} > 0, \quad (3)$$

Parameters of potential and geometry of H<sub>2</sub>O and N<sub>2</sub>O molecules

H <sub>2</sub> O		N <sub>2</sub> O	
parameters	values	parameters	values
$\sigma$ , nm	0.3234	–	–
$\epsilon$ , eV	0.007935	–	–
$r_{\text{OH}}$ , nm	0.09572	$r_{\text{ON}}$ , nm	0.186
$\Delta_{\text{HOH}}$ , deg	104.52	$\Delta_{\text{NON}}$ , deg	180
$q_{\text{O}}$ , e	0	$q_{\text{N1}}$ , e	0.279
$q_{\text{H}}$ , e	0.5190	$q_{\text{N2}}$ , e	–0.065
$q_{\text{M}}$ , e	–1.0380	$q_{\text{O}}$ , e	–0.213
$d$ , D	1.848	$d$ , D	0.396
$\alpha$ , Å <sup>3</sup>	1.4440	$\alpha$ , Å <sup>3</sup>	3.1

where the differential of free energy  $G$  is set by the equality  $dG = -SdT - pdV + \mu dn$  ( $\mu$  is the chemical potential and  $n$  is the number of molecules in a cluster). Excess (with respect to the ideal gas) free energy of clusters  $\Delta G$  was calculated in accordance with the procedure proposed in [3]. In order to determine how adequate is the model used in this work, we calculated the  $\Delta G$  energy of extended system represented by 54 water molecules in a cubic cell at whose boundaries the periodic boundary conditions were preset. As a result, satisfactory agreement (within 15%) with the data reported in [3] was reached for the  $\Delta G$  value.

In a general case, the relationship between applied electric field  $\mathbf{E}(\omega)$  and average induced dipole moment  $\mathbf{M}(\omega)$  is given by expression [4]

$$\mathbf{M}(\omega) = \frac{i\omega}{4\pi} [1 - \epsilon(\omega)] \mathbf{E}(\omega). \quad (4)$$

The dielectric permittivity's subscripts  $P$  and  $T$  are omitted in expression (4). Since the dielectric permittivity can be expressed as

$$\epsilon(\omega) = \epsilon'(\omega) + i\epsilon''(\omega), \quad (5)$$

the cluster stability with respect to the variations of electric field is determined by the  $\epsilon''(\omega)\omega/4\pi$  value, which acts as a generalized susceptibility. The inverse value is the dielectric stability coefficient. Then, the stability condition with respect to perturbations of electric field in a cluster can be expressed as

$$4\pi/[\epsilon''(\omega)\omega] > 0. \quad (6)$$

The peculiarity of this condition is that the stability of dielectric state depends on the frequency of cooperative vibrations of molecules; in the presence of external field, on the frequency of electromagnetic vibrations. It is reasonable to consider the applicability of condition (6) at a certain characteristic frequency. The frequency corresponding to the maximum of  $\epsilon''(\omega)$  was chosen as such a value.

## COMPUTER MODEL

In this work, we employed the improved interaction potential of water molecules elaborated for a rigid four-center model [5]. The geometry of monomer in this model is constructed based on the experimental data for the bond length of a molecule in the gaseous phase [6]. Fixed charges are assigned to H atoms and point  $M$  lying on the bisectrix of HOH angle at a distance of 0.0215 nm from the oxygen atom. The values of charges and the position of point  $M$  were chosen such as to reproduce both the experimental values of dipole and quadrupole moments [7, 8], as well as the calculated *ab initio* energy of a dimer and characteristic distances in the dimer [9]. Major parameters of a model and the electric properties of the gaseous phase are listed in the table. Parameters of Lennard-Jones potential introduced to account for short-range interactions are assigned to the oxygen atom. In addition to the electric charge, the polarizability that is necessary to describe the nonadditive polarization energy was also assigned to point  $M$ .

The N<sub>2</sub>O molecule is linear and can be represented in the form of three-center model with parameters shown in the table. Note the asymmetry of this molecule with respect to electric charges located in the residence of nitrogen atoms. Calculations performed using the Hartree–Fock wave functions [10, 11] demonstrated that one of these charges is positive, whereas the second one is characterized by a small negative value.

The total interaction energy of a system formed by water molecules is written as

$$U_{\text{tot}}^{(1)} = U_{\text{pair}} + U_{\text{pol}}, \quad (7)$$

where the pair-additive part of potential represents the sum of Lennard-Jones and Coulombic interactions

$$U_{\text{pair}} = \sum_i \sum_j 4\epsilon \left[ \left( \frac{\sigma_{ij}}{r_{ij}} \right)^{12} - \left( \frac{\sigma_{ij}}{r_{ij}} \right)^6 \right] + \frac{q_i q_j}{r_{ij}}. \quad (8)$$

Here,  $r_{ij}$  is the distance between points  $i$  and  $j$ ,  $q$  is the charge,  $\sigma$  and  $\epsilon$  are parameters of the Lennard-Jones potential.

Nonadditive polarization energy is determined by the relation

$$U_{\text{pol}} = -\frac{1}{2} \sum_i \mathbf{d}_i \cdot \mathbf{E}_i^0, \quad (9)$$

where  $\mathbf{E}_i^0$  is the strength of electric field in point  $i$  induced by fixed charges in point  $i$  in a system

$$\mathbf{E}_i^0 = \sum_{j \neq i} \frac{q_j \mathbf{r}_{ij}}{r_{ij}^3}. \quad (10)$$

$\mathbf{d}_i$  represents the induced dipole moment of an atom in point  $i$  and is determined as

$$\mathbf{d}_i = \alpha_i \mathbf{E}_i, \quad (11)$$

where

$$\mathbf{E}_i = \mathbf{E}_i^0 + \sum_{j \neq i} \mathbf{T}_{ij} \cdot \mathbf{d}_j. \quad (12)$$

Here,  $\mathbf{E}_i$  denotes the strength of total electric field in the point of atom  $i$  residence,  $\alpha$  is the atomic polarizability, and  $\mathbf{T}_{ij}$  is the dipole tensor

$$\mathbf{T}_{ij} = \frac{1}{r_{ij}^3} \left( \frac{3\mathbf{r}_{ij}\mathbf{r}_{ij}}{r_{ij}^2} - \mathbf{1} \right). \quad (13)$$

To calculate induced dipole moments at each time step, we used the standard iteration procedure consisting of the following steps: (a) the strength of electric field is calculated by Eq. (10) in point  $i$  induced by fixed charges in a system; (b) a certain strength of electric field is then used [Eq. (11)] to generate the initial estimates of induced dipole moments; and (c) the value of the strength of total electric field is finally calculated by Eq. (12). Steps (b) and (c) are repeated until the change of induced dipole moments between two consecutive iterations becomes smaller than the preset value. Usually, an accuracy of determining  $\mathbf{d}_i$  is taken within the  $10^{-5}$ – $10^{-4}$  D [5] range.

The description of impurity–water and impurity–impurity interactions is based on atom–atom potentials calculated [10] by applying the Gordon–Kim theory to atomic pairs represented by spherically averaged electron density of atoms. In this case, the interaction energy is determined in the following form:

$$U_{\text{tot}}^{(2)} = U_{\text{rep}} + U_{\text{disp}} + U_{\text{el}} + U_{\text{pol}}. \quad (14)$$

The energy of repulsion  $U_{\text{rep}}$  arises at short distances because of the overlap of wave functions of monomer electrons and is set by the following approximation [11]:

$$U_{\text{rep}}(r) = \sum_{i,j} b_i b_j \exp[-(c_i + c_j)r], \quad (15)$$

where the values of parameters  $b_i$  and  $c_i$  for chemical elements with outer  $p$ -electrons are reported in [11].

Dispersion energy

$$U_{\text{disp}} = -\sum_{i,j} a_i a_j r^{-6} \quad (16)$$

represents the contributions from interactions at long distances and is significant for both apolar and polar molecules. Coefficients  $a_i$  are taken from [11].

The energy of electrostatic interaction  $U_{\text{el}}$  is determined by the Coulombic interaction between the charged centers representing  $\text{H}_2\text{O}$  and  $\text{N}_2\text{O}$  molecules. The account of the interaction energy of induced electric moments of the molecules of impurity and water is performed as in calculating water–water interactions, i.e., via the polarization energy.

In order to integrate equations of motion of the centers of molecule inertia, we employed the fourth-order Gear method [12]. Time step  $\Delta t$  of integration was

equal to  $10^{-17}$  s. In the molecular dynamics calculation with time  $10^6 \Delta t$ , the equilibrium state at  $T = 233$  K was preliminarily created for water clusters containing no impurity molecules. Then, three calculation seances were performed at the same temperature. In the first case, physical properties of  $(\text{H}_2\text{O})_n$  clusters were calculated; in the second case,  $(\text{N}_2\text{O})_2(\text{H}_2\text{O})_n$ ; and in the third case,  $(\text{N}_2\text{O})_m(\text{H}_2\text{O})_9$ .

The preparation for the second-type calculations included the following. The axis of adding  $\text{N}_2\text{O}$  molecules was originally directed toward the center of inertia of  $(\text{H}_2\text{O})_n$  cluster. Two  $\text{N}_2\text{O}$  molecules were added to  $(\text{H}_2\text{O})_n$  cluster in a symmetric manner; i.e., each molecule was located on the imaginary axis penetrating water cluster through the center of inertia on the opposite sides of a cluster. In this case, the shortest distance between atoms in the  $\text{N}_2\text{O}$  molecule and atoms of water molecules did not exceed 0.5 nm. The  $\text{N}_2\text{O}$  molecule was oriented so that the nitrogen atom characterized by the negative electric charge was located closer to the surface of  $(\text{H}_2\text{O})_n$  cluster. In the studies of third type, the calculation began with the addition of  $m$   $\text{N}_2\text{O}$  molecules to  $(\text{H}_2\text{O})_9$  cluster so that the distance between the nearest atoms of dissimilar molecules did not exceed 0.6 nm. For the even number of  $\text{N}_2\text{O}$  molecules, they were arranged around a water core in a symmetric manner. In other words, the initial configuration resembles the “coil” of water molecules located in the origin of the Cartesian coordinate system with  $\text{N}_2\text{O}$  molecules on the coordinate axes. If the number of  $\text{N}_2\text{O}$  molecules exceeds six, the next molecules of impurity were located at the axes of coordinate system turned at  $45^\circ$  in the direction of spherical angles with respect to initial coordinate system.

Further evolution time of each cluster varied from 20 to 30 ps, i.e.,  $(2-3) \times 10^6 \Delta t$ . The analytical solution of equations of motion for the rotation of molecules was performed using the Rodrigo–Hamilton parameters [13]; the integration scheme of the equations of motion with rotations corresponded to the approach proposed by Sonnenschein [14]. Calculations were performed using a PENTIUM-IV computer with processor clock frequency of 1.8 GHz. About 14 h of computer time was spent for the calculation (during  $10^6 \Delta t$ ) of a cluster composed of 20 molecules.

## THERMAL AND MECHANICAL CRITERIA OF STABILITY

Thermal (1) and mechanical (2) criteria of stability are usually employed to identify the states of extended phases [1]. Even in this case, predictions made according to criterion (2) are more adequate. The system can be stable according to one criterion and unstable, in accordance with the other. Calculation formulas for heat capacity  $c_p$  and isothermal compressibility  $\beta_T$  used under these conditions of stability are reported in [15, 16].

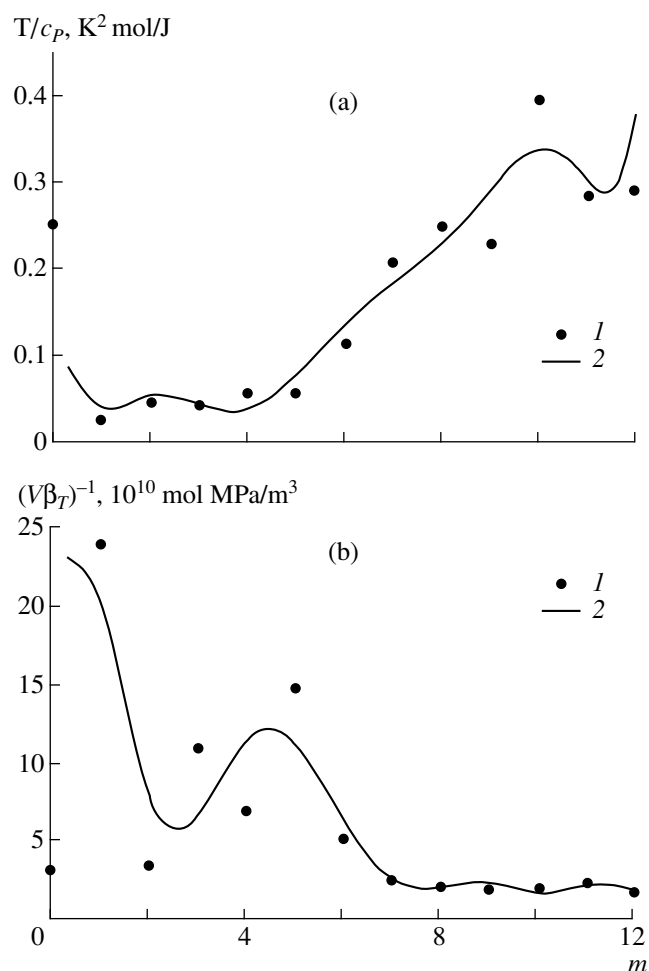


**Fig. 1.** (a) Thermal and (b) mechanical stability coefficients of  $(\text{N}_2\text{O})_m(\text{H}_2\text{O})_9$  clusters as a function of  $m$ : (1) the molecular dynamics calculation and (2) the polynomial approximation.

In the case of  $(\text{N}_2\text{O})_m(\text{H}_2\text{O})_9$  clusters, the stability coefficient  $T/c_p$  first decreases from 0.1 to 0.025 with an increase in the number of  $\text{N}_2\text{O}$  molecules, then remains almost constant up to  $m = 5$ , and increases at  $m > 5$  (Fig. 1). The criterion determined by  $1/(V\beta_T)$  has a high maximum in the  $0 \leq m \leq 2$  range; the second peak is observed on  $2 < m < 7$  portion of the curve; low values of this criterion appears at  $m \geq 7$ . In this case, the thermal criterion predicts a high stability of clusters at  $m = 0$  and  $m > 5$ ; the mechanical criterion, their highest stability at  $m = 1$  and 5.

For  $(\text{H}_2\text{O})_n$  clusters, the  $T/c_p(n)$  function decreases in a wave-like manner with increasing  $n$  (Fig. 2). In the case of  $(\text{N}_2\text{O})_2(\text{H}_2\text{O})_n$  clusters, the value of this function first decreases with an increase in  $n$  from  $n = 2$  to 5. Further, this value remains almost constant up to  $n = 13$  and starts to increase upon further rise in the number of water molecules in the cluster. Coefficient  $1/(V\beta_T)$  for  $(\text{H}_2\text{O})_n$  clusters increases until  $n$  reaches the value of 5; then it remains constant up to  $n = 13$  and

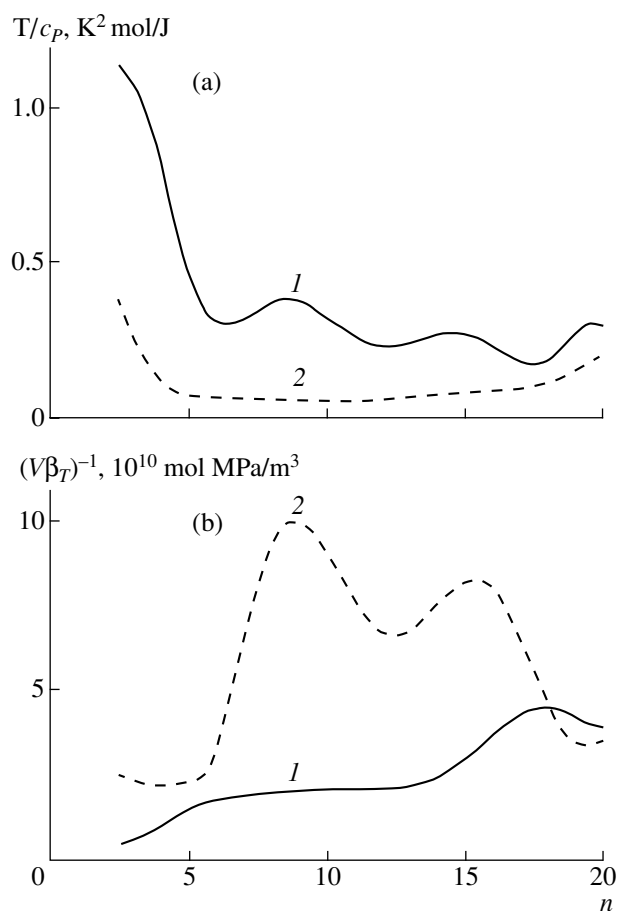


**Fig. 2.** (a) Thermal and (b) mechanical stability coefficients of clusters as a function of  $n$ : (1)  $(\text{H}_2\text{O})_n$  and (2)  $(\text{N}_2\text{O})_2(\text{H}_2\text{O})_n$  clusters.

increases again at  $n > 13$ . For  $(\text{N}_2\text{O})_2(\text{H}_2\text{O})_n$  clusters, the  $1/(V\beta_T(n))$  dependence has two peaks at  $n = 9$  and 15. At  $n > 15$ , the mechanical stability of heteroclusters decreases. In the case of  $(\text{N}_2\text{O})_2(\text{H}_2\text{O})_n$  clusters, the values of  $T/c_p$  and  $1/(V\beta_T)$  are low reliable due to large fluctuations of the second derivatives with respect to thermodynamic potential at small  $n$  values. However, already at  $n > 9$ , they can be used [17] to estimate cluster stability. Thus, the thermal criterion of stability predicts the deterioration of stability for  $(\text{H}_2\text{O})_n$  clusters with an increase in  $n$  (beginning with  $n = 9$ ) and some increase in stability for  $(\text{N}_2\text{O})_2(\text{H}_2\text{O})_n$  clusters (beginning with  $n = 11$ ).

On the contrary, the mechanical criterion of stability exhibits an increase in stability for  $(\text{H}_2\text{O})_n$  clusters and its decrease for  $(\text{N}_2\text{O})_2(\text{H}_2\text{O})_n$  aggregates within the same ranges of  $n$ . A decrease in  $1/(V\beta_T)$  value at such  $n$  values occurs due to the growth of cluster volume. In turn, an increase in the volume is associated with a significant displacement of single water molecules from the center of inertia. This situation is depicted in Fig. 3 presenting the final configuration of  $(\text{N}_2\text{O})_2(\text{H}_2\text{O})_{14}$  cluster. During the period of  $\sim 25$  ps, the  $\text{N}_2\text{O}$  molecules

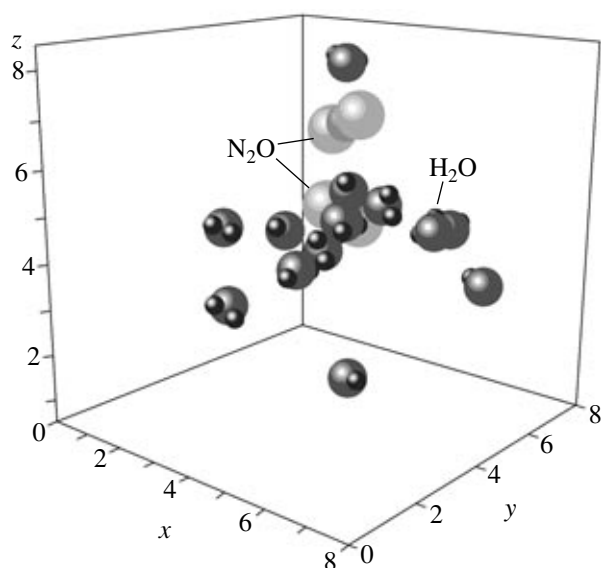


**Fig. 3.** Configuration of  $(\text{N}_2\text{O})_2(\text{H}_2\text{O})_{14}$  cluster. Coordinates of molecules are represented in units of the parameter of water–water interaction potential ( $\sigma = 0.3234$  nm).

in a cluster displaced much closer to each other. At the same time, single  $\text{H}_2\text{O}$  molecules (Fig. 3, bottom part) are moved far from the center of inertia. More realistic representation of cluster stability is given by the stability criterion (3) that responded to the variations in the number of molecules in a small formation.

#### THERMODYNAMIC CRITERION OF CLUSTER STABILITY

According to calculations,  $(\text{N}_2\text{O})_m(\text{H}_2\text{O})_9$  clusters are stable when the number of  $\text{N}_2\text{O}$  molecules does not exceed two. Positive values of the second derivative

$\left(\frac{\partial^2 G}{\partial n^2}\right)_{P,T}$  are replaced at  $m \leq 2$  by the  $3 \leq m \leq 7$  range

(Fig. 4a), where this criterion of stability is sign-variable and has low values. This is the “transitive” region from the stable states to the unstable ones and vice versa. The state of clusters with  $m \geq 8$  can be characterized as absolutely thermodynamically unstable. In this region, the coefficient of stability (3) drops still lower toward the range of negative values with an increase in the number of  $\text{N}_2\text{O}$  molecules.

Close relationship is observed between the behavior of the coefficient of stability (3) and the variation of the ratio between self-diffusion coefficient  $D$  of molecules in clusters. The self-diffusion coefficient was determined via the mean-square displacements of the centers of inertia for molecules. At  $m \leq 2$ , the  $D$  values for  $\text{N}_2\text{O}$  molecules are larger than for water molecules (Fig. 4b). Low values of coefficient  $D$  for water molecules fit the region of cluster stable states. When the cluster states first fit the transitive region and then the

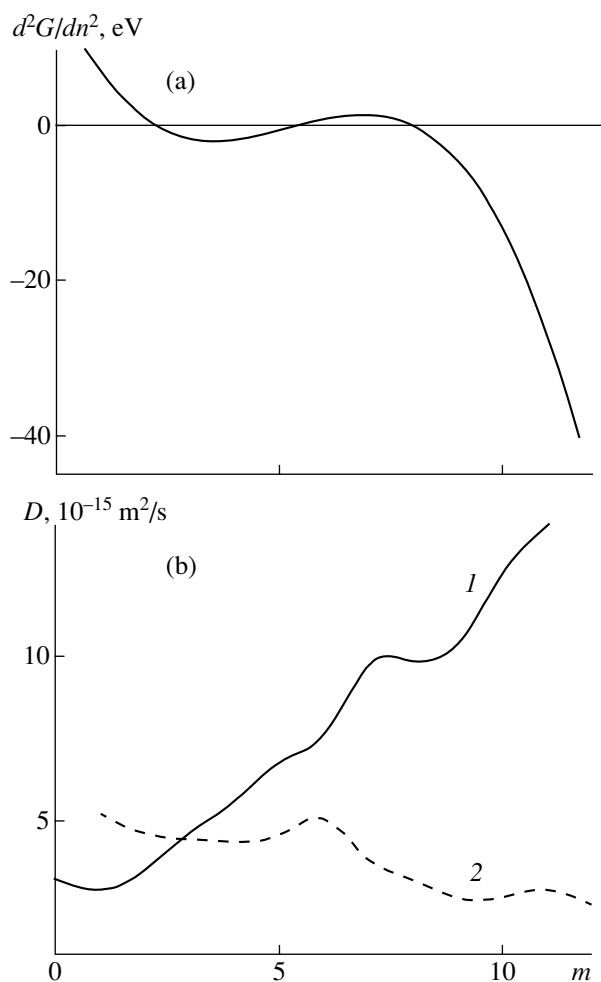


**Fig. 4.** (a) Second derivative of free energy with respect to the number of molecules and (b) self-diffusion coefficients in the  $(\text{N}_2\text{O})_m(\text{H}_2\text{O})_9$  cluster as a function of  $m$ : (1) for  $\text{H}_2\text{O}$  and (2) for  $\text{N}_2\text{O}$  molecules.

region of unstable states, coefficient  $D$  for water molecules becomes larger than the self-diffusion coefficient of  $\text{N}_2\text{O}$  molecules.

According to criterion (3), at 233 K, the  $(\text{H}_2\text{O})_n$  clusters are thermodynamically stable within the  $2 \leq n \leq 10$  size range, whereas  $(\text{N}_2\text{O})_2(\text{H}_2\text{O})_n$  clusters are stable only at  $n \geq 5$  (Fig. 5a). Our calculations performed for water clusters at the same temperature, using three-center model SPCE/POL1 [18] and procedure SHAKE [19] restoring the shape of water molecule, demonstrated that the  $(\text{H}_2\text{O})_n$  aggregates with  $2 \leq n \leq 12$  are stable. The self-diffusion coefficient of water molecules in  $(\text{N}_2\text{O})_2(\text{H}_2\text{O})_n$  clusters at  $n < 5$  is larger than the  $D$  value for  $\text{N}_2\text{O}$  molecules belonging to these clusters (Fig. 5b). This is the region of unstable states. At  $n \geq 5$ , the situation changes so that  $D_{\text{H}_2\text{O}} < D_{\text{N}_2\text{O}}$  and clusters become thermodynamically stable. Thus, the values of the coefficient of thermodynamic stability correlate with the kinetic properties of heterocluster molecules.

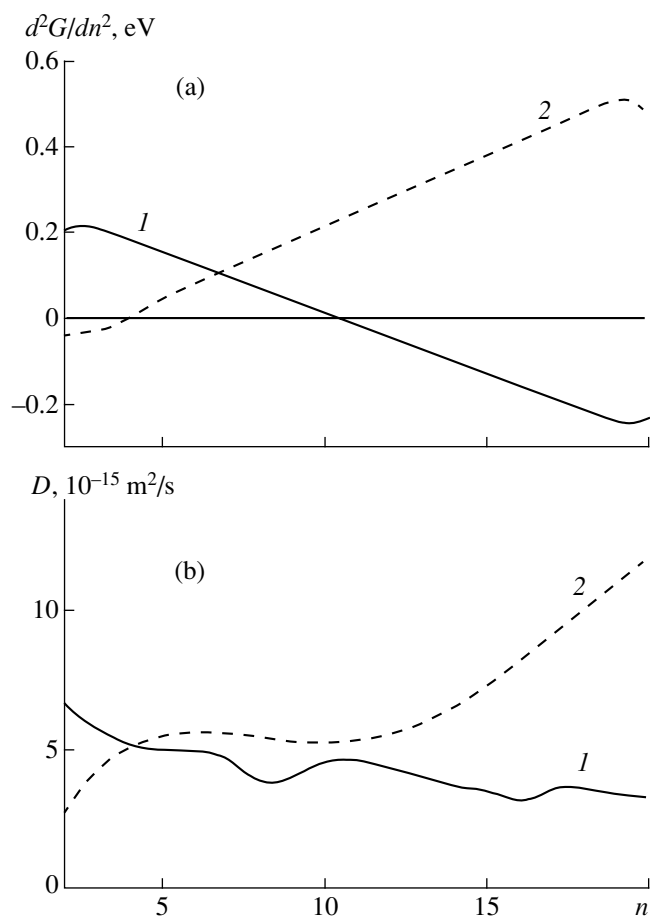


**Fig. 5.** (a) Second derivative of free energy with respect to the number of molecules in clusters: (1)  $(\text{H}_2\text{O})_n$  and (2)  $(\text{N}_2\text{O})_2(\text{H}_2\text{O})_n$  and (b) self-diffusion coefficients of molecules in the  $(\text{N}_2\text{O})_2(\text{H}_2\text{O})_n$  cluster: (1)  $\text{H}_2\text{O}$  and (2)  $\text{N}_2\text{O}$  molecules.

#### DIELECTRIC PERMITTIVITY OF $(\text{H}_2\text{O})_n$ AND $(\text{N}_2\text{O})_2(\text{H}_2\text{O})_n$ CLUSTERS

Static electric constant  $\epsilon_0$  was calculated via the fluctuations of total dipole moment  $\mathbf{M}$  [20]

$$\epsilon_0 - 1 = \frac{4\pi}{3VkT} [\langle \mathbf{M}^2 \rangle - \langle \mathbf{M} \rangle^2]. \quad (17)$$

Let us introduce the Fourier–Laplace transform of function  $f$  via the relation

$$L_{i\omega}[f] = \int_0^{\infty} dt e^{-i\omega t} f(t) \quad (18)$$

and the normalized autocorrelation function of the  $\mathbf{M}$  value, using equality

$$\Phi(t) = \langle \mathbf{M}(0) \cdot \mathbf{M}(t) \rangle / \langle \mathbf{M}^2 \rangle. \quad (19)$$

The relationship between the frequency-dependent electric constant and the Fourier–Laplace transform for

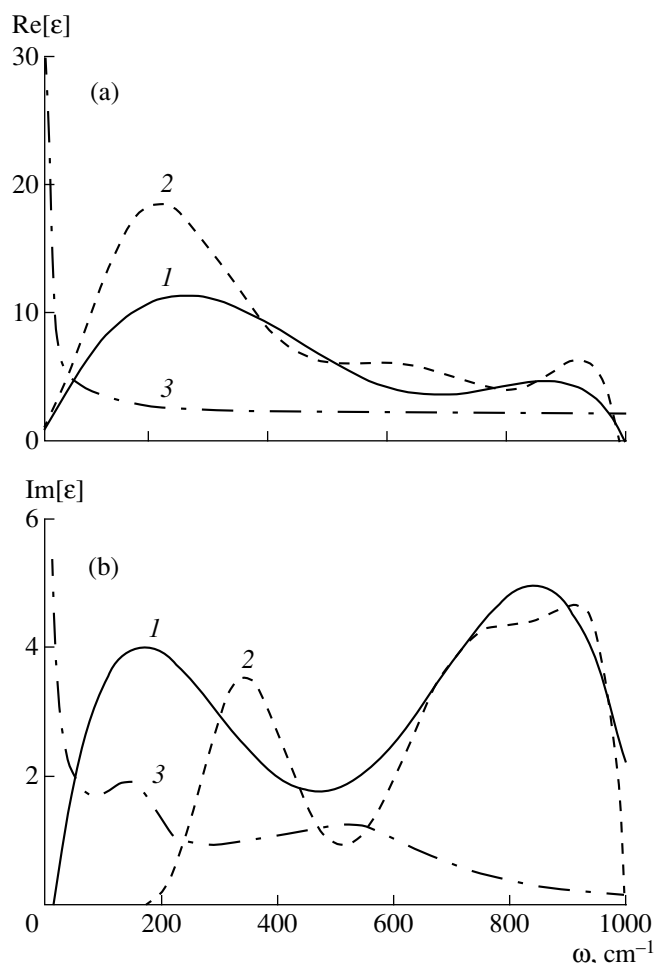


**Fig. 6.** Frequency dependences of (a) real and (b) imaginary parts of dielectric permittivity of (1)  $(\text{H}_2\text{O})_{12}$  and (2)  $(\text{N}_2\text{O})_2(\text{H}_2\text{O})_{12}$  clusters, (3): (a) molecular dynamics calculation for bulk water with the MCY potential [21] and (b) experimental results for bulk water [22, 23].

the derivative of function  $\Phi$  with respect to time is given by expression [20]

$$L_{i\omega}[-\dot{\Phi}] = \frac{\epsilon(\omega) - 1}{\epsilon_0 - 1} = 1 - i\omega L_{i\omega}[\Phi]. \quad (20)$$

The  $\epsilon_0$  value is determined via function  $\epsilon(\omega)$ :  $\epsilon_0 = \epsilon(0)$ .

Calculated frequency distributions of dielectric permittivity for  $(\text{H}_2\text{O})_n$  and  $(\text{N}_2\text{O})_2(\text{H}_2\text{O})_n$  clusters demonstrate that both real  $\epsilon'(\omega)$  and imaginary  $\epsilon''(\omega)$  parts of spectra are always characterized by two or one peak. Direct relationship between the number of peaks and cluster size is not observed. Figure 6 illustrates the real and imaginary parts of spectra for the dielectric permittivity of the clusters containing 12 water molecules, as well as the corresponding spectra for the bulk water. The  $\epsilon(\omega)$  function of extended system was calculated using model MCY for water [21] that does not account for the molecule polarizability. Rapid decrease of the intensity of this spectrum fits the frequency range of 2 ≤

$\omega \leq 100 \text{ cm}^{-1}$ . The  $\epsilon'(\omega)$  spectrum for  $(\text{H}_2\text{O})_n$  clusters is bimodal. Maxima fit frequencies  $\omega_1 \approx 215 \text{ cm}^{-1}$  and  $\omega_2 \approx 847 \text{ cm}^{-1}$ . As the size of such a cluster increases due to the addition of two polar molecules ( $\text{N}_2\text{O}$ ), the  $\epsilon'(\omega)$  spectrum is deformed. The intensity of the first maximum increases by a factor of 1.64, reaching the value of  $\epsilon' \approx 18.9$  at a permanent position of this peak ( $215 \text{ cm}^{-1}$ ). The second peak of spectrum  $\epsilon'(\omega)$  in  $(\text{N}_2\text{O})_2(\text{H}_2\text{O})_n$  cluster shifts to the right ( $\omega_2 \approx 910 \text{ cm}^{-1}$ ) and its height increases also. In this case, the shoulder is formed between the peaks in spectrum  $\epsilon'(\omega)$ .

Imaginary  $\epsilon''(\omega)$  parts of corresponding frequency distributions are compared in Fig. 6b with the experimentally measured spectrum of dielectric relaxation for bulk water [22, 23]. The  $\epsilon''(\omega)$  spectrum for water has the mode of relaxation type with a frequency of less than  $10 \text{ cm}^{-1}$ , as well as two low maxima at  $\omega_1 \approx 150 \text{ cm}^{-1}$  and  $\omega_2 \approx 550 \text{ cm}^{-1}$ . There is no low-frequency mode in the spectra of dielectric relaxation for the clusters; however, two pronounced peaks appear. Furthermore, the intensity of the second peak is higher than that of the first one. Bresme believes [20] the appearance of the first peak in the  $\epsilon''(\omega)$  spectrum is due to the use of polarizable molecules model. Peak positions for  $(\text{H}_2\text{O})_n$  clusters correspond to frequencies of 150 and  $850 \text{ cm}^{-1}$ , whereas for  $(\text{N}_2\text{O})_2(\text{H}_2\text{O})_n$  clusters, these frequencies are equal to 340 and  $910 \text{ cm}^{-1}$ . The  $\epsilon''(\omega)$  spectrum of heterocluster is characterized, in addition to the shift of maxima, by the appearance of the shoulder to the left of the second maximum. Thus, the addition of  $\text{N}_2\text{O}$  molecules leads to the deformation of the dielectric relaxation spectrum of clusters; moreover, the significant change of  $\epsilon''$  value occurs at higher frequencies. The largest shift to the right is observed for the first characteristic relaxation frequency.

### THE STABILITY OF CLUSTERS TO ELECTRIC PERTURBATIONS

The stability of dielectric medium formed by a cluster is characterized by Fig. 7. Frequency  $\omega_E$ , corresponding to the largest system response, oscillates with the variation of cluster size (Fig. 7a). In the case of  $(\text{H}_2\text{O})_n$  clusters, the largest values of frequency of field  $\mathbf{E}$  corresponding to maximal perturbations of dielectric properties are observed at  $n = 3, 11,$  and  $16$ ; minima of frequency  $\omega_E$ , at  $n = 6, 8,$  and  $12$ . The highest frequencies  $\omega_E$  resulted in similar effects for  $(\text{N}_2\text{O})_2(\text{H}_2\text{O})_n$  clusters correspond to  $n = 2, 7, 10\text{--}12,$  and  $16$ ; minima of  $\omega_E$  correspond to  $n = 4, 9, 13,$  and  $18$ . In general, at  $n > 6$ , the  $\omega_E(n)$  curve for  $(\text{N}_2\text{O})_2(\text{H}_2\text{O})_n$  clusters follows the trend of corresponding curve for  $(\text{H}_2\text{O})_n$  aggregates albeit with lower amplitude. At small  $n$  ( $n < 6$ ), these curves are out of phase.

Stability coefficient  $4\pi/[\epsilon''(\omega)\omega]$  of dielectric properties (Fig. 7b) demonstrates a higher stability of  $(\text{N}_2\text{O})_2(\text{H}_2\text{O})_n$  clusters at  $n < 13$  and  $n > 18$  relative to  $(\text{H}_2\text{O})_n$  clusters. In the  $13 \leq n \leq 18$  size range, the values of the coefficient of stability (6) are comparable for

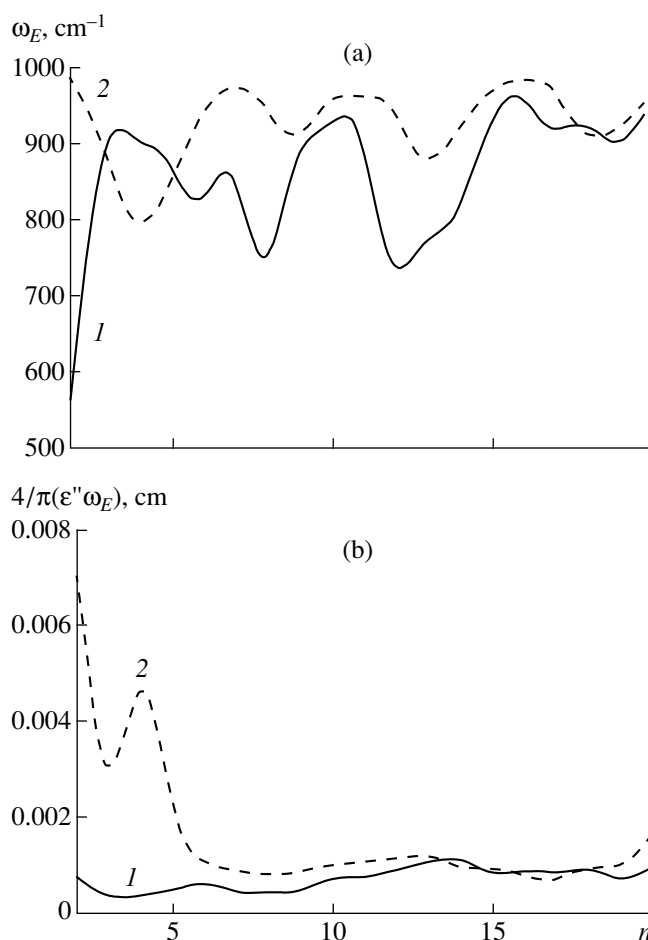


**Fig. 7.** Dependences of (a) frequency  $\omega_E$  and (b) the criterion of cluster stability on the size  $n$  of clusters: (1)  $(\text{H}_2\text{O})_n$  and (2)  $(\text{N}_2\text{O})_2(\text{H}_2\text{O})_n$ .

these clusters. For the smallest heteroclusters under consideration ( $n < 5$ ), the stability coefficient of dielectric properties has the largest values in the cases where the thermodynamic criterion of stability (3) is negative; i.e., where the perturbation of a system state due to the addition to or the removal of only one molecule leads to the buildup of instability. This is related to the fact that thermodynamically unstable, destroying clusters response very weakly to the variations of electric field.

### CONCLUSIONS

The results obtained are important for the adequate estimation of greenhouse effect. In particular, the data on cluster stability are required for understanding the heat exchange between incident solar radiation and backward infrared Earth radiation. It is known that the infrared radiation is most intensely absorbed by water vapors. As a result of intense absorption by the atmosphere, only small portion of Earth radiation leaves the atmosphere, thus preventing the Earth cooling. The enhancement of greenhouse effect related to the accu-

mulation of greenhouse gases such as CO<sub>2</sub>, CH<sub>4</sub>, and N<sub>2</sub>O can lead to unfavorable climatic variations. Ultradispersed aqueous medium is present both in the troposphere and in the lower stratosphere [24]. At low temperatures, the growth of clusters should be associated with the entrapment of impurity molecules.

In this work, it was shown that (H<sub>2</sub>O)<sub>n</sub> clusters beginning with  $n \geq 5$  are capable of entrapping up to two N<sub>2</sub>O molecules with no loss of stability. The thermodynamic stability of heteroclusters is ensured by their structure (N<sub>2</sub>O molecules in these clusters tend to accumulate in the vicinity of the center of inertia), as well as by their kinetic properties (in stable clusters, the self-diffusion coefficient is smaller for water molecules than for nitrogen oxide molecules). The addition of two N<sub>2</sub>O molecules to water clusters leads to a substantial shift of the first characteristic frequency of dielectric relaxation to the right; i.e., the relaxation processes of electric properties proceed at higher frequencies. In general, heteroclusters are more stable to the variations of external electric field than clusters with the same number of water molecules.

Thus, under the troposphere conditions, water clusters represent "viable" formations that exist (up to certain sizes) in the form of molecular or heteromolecular ensembles. The entrapment of two N<sub>2</sub>O polar molecules by the water aggregate composed of seven or more molecules leads to an increase in the cluster stability, thus increasing the probability of its further growth. The contribution of cluster (heterocluster) to the absorption of Earth radiation is comparable with the absorption of this radiation by a monomer. A decrease in the monomer fraction due to the clusterization of atmospheric greenhouse gases favors the reduction of greenhouse effect.

#### ACKNOWLEDGMENTS

This work was supported by the Russian Foundation for Basic Research, project no. 03-02-96807-Yugra.

#### REFERENCES

1. Semenchenko, V.K., *Izbrannye glavy teoreticheskoi fiziki* (Selected Chapters of Theoretical Physics), Moscow: Prosveshchenie, 1966.

2. Shevkunov, S.V., *Kolloidn. Zh.*, 2002, vol. 64, no. 2, p. 262.
3. Hermans, J., Pathiaseril, A., and Anderson, A., *J. Am. Chem. Soc.*, 1988, vol. 110, p. 5982.
4. Kuni, F.M., *Statisticheskaya fizika i termodinamika* (Statistical Physics and Thermodynamics), Moscow: Nauka, 1981.
5. Dang, L.X. and Chang, T.-M., *J. Chem. Phys.*, 1997, vol. 106, p. 8149.
6. Benedict, W.S., Gailar, N., and Plyler, E.K., *J. Chem. Phys.*, 1956, vol. 24, p. 1139.
7. Xantheas, S., *J. Chem. Phys.*, 1996, vol. 104, p. 8821.
8. Feller, D. and Dixon, D.A., *J. Chem. Phys.*, 1996, vol. 100, p. 2993.
9. Smith, D.E. and Dang, L.X., *J. Chem. Phys.*, 1994, vol. 100, p. 3757.
10. Spackman, M.A., *J. Chem. Phys.*, 1986, vol. 85, p. 6579.
11. Spackman, M.A., *J. Chem. Phys.*, 1986, vol. 85, p. 6587.
12. Haile, J.M., *Molecular Dynamics Simulation. Elementary Methods*, New York: Wiley, 1992.
13. Koshlyakov, V.N., *Zadachi dinamiki tverdogo tela i prikladnoi teorii giroskopov* (Problems of Solid Body Dynamics and Applied Theory of Gyroscopes), Moscow: Nauka, 1985.
14. Sonnenschein, R., *J. Comput. Phys.*, 1985, vol. 59, p. 347.
15. Galashev, A.E., Pozharskaya, G.I., and Chukanov, V.N., *Zh. Strukt. Khim.*, 2002, vol. 43, no. 3, p. 494.
16. Galashev, A.E., Chukanov, V.N., and Pozharskaya, G.I., *Zh. Strukt. Khim.*, 2002, vol. 43, no. 3, p. 486.
17. Galashev, A.E., Sigon, F., and Servida, A., *Zh. Strukt. Khim.*, 1997, vol. 38, no. 6, p. 1092.
18. Caldwell, J., Dang, L.X., and Kollman, P.A., *J. Am. Chem. Soc.*, 1990, vol. 112, p. 9144.
19. Ryckaert, J.-P., Ciccotti, G., and Berendsen, H.J.C., *J. Comput. Phys.*, 1977, vol. 23, p. 327.
20. Bresme, F., *J. Chem. Phys.*, 2001, vol. 115, p. 7564.
21. Neumann, M., *J. Chem. Phys.*, 1985, vol. 82, p. 5663.
22. Angell, C.A. and Rodgers, V., *J. Chem. Phys.*, 1984, vol. 80, p. 6245.
23. Hasted, J.B., Husain, S.K., Frescura, F.A.M., and Birch, J.R., *Chem. Phys. Lett.*, 1984, vol. 118, p. 622.
24. Galashev, A.E., Pozharskaya, G.I., and Chukanov, V.N., *Kolloidn. Zh.*, 2002, vol. 64, no. 6, p. 762.